On the quenching of excited electronic states of molecular nitrogen in nanosecond pulsed discharges in atmospheric pressure air

M. S. Bak, W. Kim, and M. A. Cappelli

ARTICLES YOU MAY BE INTERESTED IN

The spectrum of molecular nitrogen
Journal of Physical and Chemical Reference Data **6**, 113 (1977); https://doi.org/10.1063/1.555546

Cross Sections for Electron Collisions with Nitrogen Molecules
Journal of Physical and Chemical Reference Data **35**, 31 (2006); https://doi.org/10.1063/1.1937426

Determination of vibrational and rotational temperatures in highly constricted nitrogen plasmas by fitting the second positive system of N_2 molecules
AIP Advances **5**, 057158 (2015); https://doi.org/10.1063/1.4921916

On the quenching of excited electronic states of molecular nitrogen in nanosecond pulsed discharges in atmospheric pressure air

M. S. Bak,[a] W. Kim, and M. A. Cappelli
Department of Mechanical Engineering, Stanford University, Stanford, California 94305-3032, USA

Emission measurements are carried out to study the quenching of excited electronic states of nitrogen, N_2^*, in nanosecond pulsed discharges in atmospheric pressure air and nitrogen. The results reveal that ground state N_2 quenches $N_2(C)$ and $N_2(B)$ at rates less than dissociative quenching by ground state O_2 by a factor of 4 and 2.5, respectively. Kinetic simulations with the inferred quench rates indicate that the dissociative quenching of N_2^* by O_2 is responsible for 82% of atomic oxygen production while electron-impact dissociation of O_2 is for 5% under these discharge conditions. © *2011 American Institute of Physics.* [doi:10.1063/1.3535986]

High repetition-rate nanosecond pulsed discharges that generate high pressure plasmas with a low power budget[1,2] have been used in combustion to extend lean flammability limits[3,4] and to reduce ignition delay times.[5] This benefit is attributed to the production of reactive atomic oxygen (O), hydrogen (H), and hydroxyl (OH) radicals.[3,6] To understand O radical production in detail, direct measurements of O radicals[7,8] as well as kinetic simulations[9] have been carried out for short-pulsed discharges in air and air/fuel mixtures. Measurements in air[8] indicate that a rapid production of O radicals follows a fast decay of electronically excited states of molecular nitrogen (N_2^*), suggesting that dissociative quenching may be the main O radical production channel. This finding is supported by previous kinetic experiments[10–12] that suggest that ground-state molecular oxygen, O_2, quenches N_2^* more effectively than molecular nitrogen, N_2. Unfortunately, most of these rate coefficients are obtained at room temperature and low pressure (a few Torr), and their temperature or pressure dependence is not well known. Therefore, the lesser role played by self quenching of N_2^* by N_2 in these highly nonequilibrated atmospheric pressure plasmas must be verified.

In this letter, we present measurements of time-resolved N_2 emission in pulsed discharges of air and pure nitrogen. The N_2 emission profiles in both air and nitrogen are found to be remarkably similar. To understand this, a zero-dimensional (0-D) kinetic simulation is carried out and a comparison of the predicted temporal behavior in the excited states of nitrogen to that measured is used to provide an estimate of the quench rate coefficients of $N_2(C)$ and $N_2(B)$ by N_2 and O_2. With the revised coefficients, the relative importance of the primary mechanisms for O radical production (dissociative quenching of each of these states of N_2 and direct electron impact dissociation) is determined.

A schematic of the experiment is shown in Fig. 1. The discharge is generated between two tungsten electrodes (1 mm diameter, 1 mm separation) connected to a high repetition pulsed power supply (FID Technology F1112) that generates Gaussian temporal voltage pulses of typically 8 kV peak, 10 ns duration, and 50 kHz repetition rate. The light emitted from the center of the discharge is collected and transmitted through an optical fiber directly to a photomultiplier tube (PMT) (Hamamatsu R928, 2.2 ns rise-time, and PMT socket, Hamamatsu E717–63, designed for fast time response) equipped with band-pass filters (Thorlabs FB340–10 or FB760–10, depending on the N_2^* band of interest), or is dispersed using a monochromator (Jarrell-Ash 82–020) with the PMT at its exit. The PMT signals used in conjunction with the band-pass filters are directly recorded and averaged over several shots by an oscilloscope (Tektronix TDS7104, 1GHz bandwidth), while the signals through the monochromator are gated and integrated through a boxcar integrator (SRS SR250) with a gate width of 2 ns, triggered and synchronized with the pulse generator using a delay generator (SRS DG535). The PMT/socket temporal response function is determined using a short pulsed light source, and the detector is found to have an overall rise-time of 2 ns, with a fall time of about 5 ns. During the measurements, either air or pure nitrogen flows through the discharge with a speed of about 4 m/s.

Time-resolved emission intensities of the $N_2(C-B)$ and $N_2(B-A)$ electronic transitions taken using the narrow band-pass filters (10 nm windows, centered about 340 and 760 nm) for discharges in air and nitrogen are shown in Figs. 2(a) and 2(b), respectively. The temporal characteristics are verified using the spectrally resolved emission taken with a monochromator. The emission follows the general shape of the applied voltage but with slower overall decay. The most surprising result is that we see little difference in the emis-
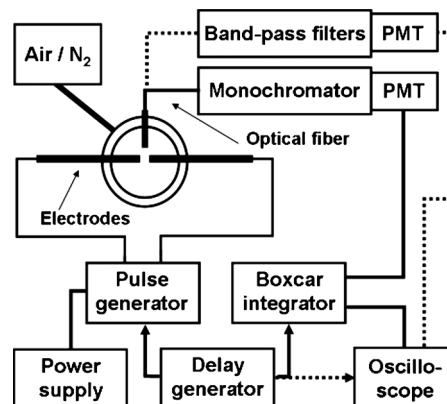

FIG. 1. Schematic of experimental setup.
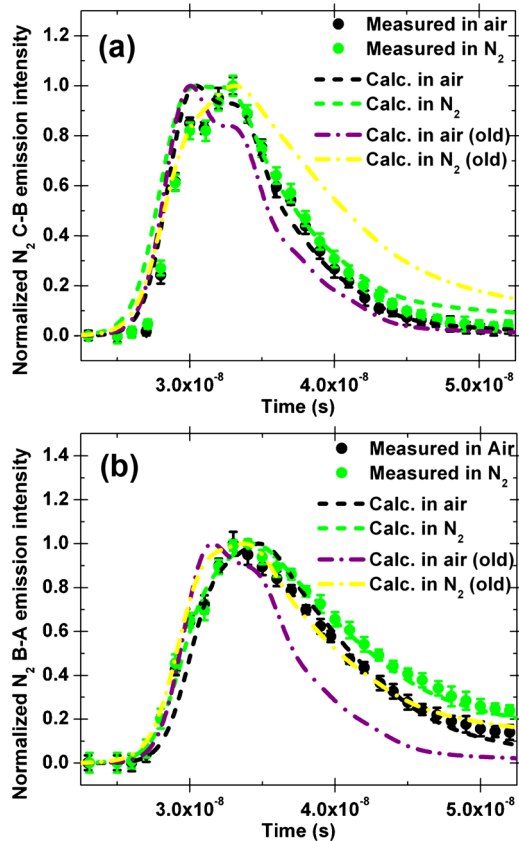
[a]Electronic mail: moonsoo@stanford.edu.

FIG. 2. (Color online) Normalized temporal emission of (a) N_2(C-B) and (b) N_2(B-A) for discharges in air and nitrogen. Symbols are measured data, and dashed and dot-dashed lines are calculated using rate coefficients proposed in this study and commonly used ones, respectively.

sion shapes (particularly the decay) between measurements in air and in nitrogen, suggesting that the presence of oxygen has little effect on the emission decay under these conditions. According to these results, any correlation between the temporal decay in the excited state emission and the rise in measured O-atom concentrations may be coincidental and is not sufficient confirmation of the importance of dissociative quenching by ground state molecular oxygen.

Time-resolved spectra of the N_2(C-B) (0,2), (1,3), and (2,4) bands for discharges in air are also recorded to study the rotational/vibrational state-specific occupancy. Figure 3
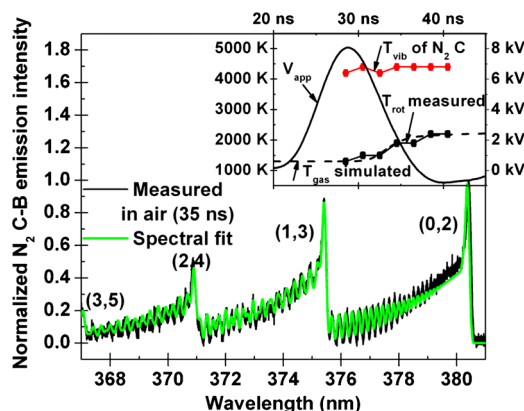

FIG. 3. (Color online) Normalized N_2(C-B) (0,2)(1,3)(2,4) emission spectrum measured in air (black) with its spectral fit (green), and calculated temporal rotational and vibrational temperatures of N_2(C) with simulated gas temperature.

shows the spectrum at the time when the emission intensity is highest with its fit obtained using a spectral line simulation. The emission is well reproduced using a spectrum synthesized with a Boltzmann distribution of rotational and vibrational states in accordance with a temperature of T_{rot} = 1900 K and T_{vib} = 4400 K, respectively. The time evolution of T_{rot} and T_{vib} are also presented in Fig. 3. T_{vib} is found to rise nearly immediately to a temperature of 4400 K while T_{rot} increases more gradually to 2200 from 1300 K during the pulse duration. This rise in rotational temperature is indicative of a slower but still rapid energy cascade into translational energy of the background gas, since the high pressure assures strong rotational-translational coupling. The initial T_{rot} of 1300 K is the result of heating from previous discharge pulses.

We have carried out 0-D kinetic simulations to understand this quenching process. We consider excited electronic states of N_2(A, B, a′, and C), ground electronic states of N_2(X), N, O_2(X), O_2(a), O_2(b), O, NO, O_3, N_2^+, N_4^+, O_2^+, and free electrons (e) in the analysis. The reaction set includes electron impact excitation, dissociation and ionization of O_2 and N_2, associative ionization, recombination of electrons and positive ions, ion conversion, direct quenching of N_2^* by N_2, dissociative quenching of N_2^* by O_2, and chemical transformation of ground state species, as described in detail in the online supplemental material.[13] The rate coefficients for collisions between neutral species and ions are adapted from previous simulations of N_2 and N_2-O_2 discharges.[14–16] Since electron impact excitation, dissociation, ionization, and electron-ion recombination processes are coupled to the electron energy distribution function, rate coefficients for these reactions are obtained through a solution of the Boltzmann equation facilitated by the use of the commercially available software, BOLSIG.[17] Only a reduced set of cross sections pertaining to elastic and inelastic collisions with the parent species (ground state N_2 and O_2) are considered.[18] The peak reduced electric field of E/n is determined to be 285 ($\pm$4) Td by matching the temporal rise in the measured gas temperature (assumed to be equal to the measured rotational temperature as shown in the inset in Fig. 3) to that simulated using an energy equation in which the energy deposited into Ohmic dissipation is equal to the energy needed to advance reactions and to increase gas temperature, in accordance with the prescription provided by Uddi.[19] The peak E/n used is smaller than the nominal estimate based on the applied voltage and gap distance, a result attributed to sheath formation across each electrodes.[20] The calculation requires an initial estimate of the electron density between discharge pulses, which we take to be the time-average electron density measured in similar experiments,[1] 10^{13} cm^{-3}. In evolving the kinetics, we assume a constant background number density of 5.6×10^{18} cm^{-3} (corresponding to a value at 1 atm and an initial temperature of 1300 K) since the pulse time-scale is shorter than that of acoustic expansion of the discharge volume.

The simulated temporal emission of the N_2(C-B) and N_2(B-A) bands in air and nitrogen (convolved with the temporal response function of the detector) is also presented in Figs. 2(a) and 2(b), respectively. With often-used quenching rates[16] for N_2^* by N_2(X) and by O_2, we calculate a faster decay of N_2(C) and N_2(B) in air than in nitrogen with notable differences between the simulated and corresponding
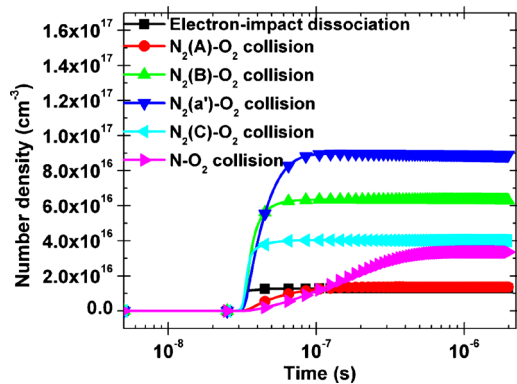
FIG. 4. (Color online) Number densities of O radicals produced through electron impact dissociation, dissociative quenching of $N_2(A)$, $N_2(B)$, $N_2(a')$, and $N_2(C)$, and $N-O_2$ collisions as functions of time.

measured curves. The quenching of $N_2(C)$ by $N_2(X)$ is underpredicted while that of $N_2(C)$ by O_2 is overpredicted. For $N_2(B)$, quenching by N_2 and O_2 are both overpredicted, presumably because the commonly used rate coefficients for $N_2(B)$ quenching[11,16] are weighted-averages over vibrational state-specific rates, which account for faster quenching of higher vibrational states. This contrasts that used for $N_2(C)$, which is based on quenching of the ground vibrational level ($v'=0$). To model our temporal emission, the rate coefficients for these quenching reactions are adjusted to obtain agreement between measured and simulated curves (black dashed lines for air and green dashed lines for nitrogen). The resulting coefficients for quenching of $N_2(C)$ by N_2 and by O_2 are found to be $2.5(\pm0.3)\times10^{-11}$ and $10(\pm0.3)\times10^{-11}$ cm^3 s^{-1}, respectively, whereas for $N_2(B)$ by N_2 and O_2 are $1.6(\pm0.3)\times10^{-11}$ and $4(\pm0.3)\times10^{-11}$ cm^3 s^{-1}, respectively. For $N_2(C)$ and $N_2(B)$ quenching by N_2, the rate coefficients needed to reproduce experiments are between the state-specific coefficients for $v'=0$ and for $v'=1, 2$.[21,22] This enhanced quenching is not unexpected, as the high vibrational temperature will result in elevated populations of excited vibrational states. In contrast, for the dissociative quenching of $N_2(C)$ and $N_2(B)$ by O_2, the rate coefficients are smaller than those commonly used by factors of 3 and 5, respectively. Since N_2^* is quenched faster in higher vibrational states by O_2,[10,11] we surmise that the lower quenching rates needed may be due to a strong pressure or temperature dependence, for which there are no experimental data.

Using the determined quenching rate coefficients of N_2^* by N_2 and O_2, we compute the evolution of O radicals produced through the two dissociation channels (dissociative quenching or direct) for a single discharge pulse (see Fig. 4).

We find that 82% of O produced is the result of dissociative quenching while electron impact dissociation is responsible for about 5%. The revised rate coefficients decrease the fraction of O radicals produced by dissociative quenching by 1%, and dissociative quenching is still the dominant channel for producing O radicals, as concluded from previous studies.[7–9] The O radical concentration produced after a single discharge pulse is found to be $2.5(\pm0.5)\times10^{17}$ cm^{-3} corresponding to a mole fraction of $4.4(\pm0.4)\times10^{-2}$.

[1] C. H. Kruger, C. O. Laux, L. Yu, D. M. Packan, and L. Pierrot, Pure Appl. Chem. **74**, 337 (2002).

[2] S. O. Macheret, M. N. Shneider, and R. B. Miles, IEEE Trans. Plasma Sci. **30**, 1301 (2002).

[3] G. P. Pilla, D. Galley, D. A. Lacoste, F. Lacas, D. Veynante, and C. O. Laux, IEEE Trans. Plasma Sci. **34**, 2471 (2006).

[4] A. Bao, Y. G. Utkin, S. Keshav, G. Lou, and I. V. Adamovich, IEEE Trans. Plasma Sci. **35**, 1628 (2007).

[5] S. V. Pancheshnyi, D. A. Lacoste, A. Bourdon, and C. O. Laux, IEEE Trans. Plasma Sci. **34**, 2478 (2006).

[6] S. M. Starikovskaia, J. Phys. D **39**, R265 (2006).

[7] M. Uddi, N. Jiang, E. Mintusov, I. V. Adamovich, and W. R. Lempert, Proc. Combust. Inst. **32**, 929 (2009).

[8] G. D. Stancu, F. Kaddouri, D. A. Lacoste, and C. O. Laux, J. Phys. D **43**, 124002 (2010).

[9] M. Uddi, N. Jiang, I. V. Adamovich, and W. R. Lempert, J. Phys. D **42**, 075205 (2009).

[10] S. V. Pancheshnyi, S. M. Starikovskaia, and A. Yu. Starikovskii, Chem. Phys. **262**, 349 (2000).

[11] L. G. Piper, J. Chem. Phys. **97**, 270 (1992).

[12] L. G. Piper, J. Chem. Phys. **87**, 1625 (1987).

[13] See supplementary material at http://dx.doi.org/10.1063/1.3535986 for reaction set used in kinetic simulations for discharge in nitrogen and air.

[14] I. A. Kossyi, A. Y. Kostinsky, A. A. Matveyev, and V. P. Silakov, Plasma Sources Sci. Technol. **1**, 207 (1992).

[15] B. F. Gordiets, C. M. Ferreira, V. L. Guerra, J. M. A. H. Loureiro, J. Nahorny, D. Pagnon, M. Touzeau, and M. Vialle, IEEE Trans. Plasma Sci. **23**, 750 (1995).

[16] M. Capitelli, C. M. Ferreira, B. F. Gordiets, and A. I. Osipov, *Plasma Kinetics in Atmospheric Gases* (Springer, Berlin, 2000).

[17] See http://www.siglo-kinema.com/bolsig.htm for SIGLO-KINEMA Software, Monument, CO.

[18] L. C. Pitchford, S. V. ONeil, and J. R. Rumble, Jr., Phys. Rev. A **23**, 294 (1981).

[19] M. Uddi, Ph.D. thesis, The Ohio State University, 2008.

[20] S. O. Macheret, M. N. Shneider, and R. C. Murray, Phys. Plasmas **13**, 023502 (2006).

[21] D. E. Shemansky, J. Chem. Phys. **64**, 565 (1976).

[22] G. Dilecce, P. F. Ambrico, and S. D. Benedictis, Plasma Sources Sci. Technol. **16**, S45 (2007).